in Proc. 7th Int. Congress for Sensors, Transducers & Systems, SENSOR'95 (Nuremberg, Germany, 1995).

GENERAL ERROR FUNCTION OF SYNTHETIC-HETERODYNE SIGNAL PROCESSING OF INTERFEROMETRIC FIBRE OPTIC SENSORS

A.B. Lobo Ribeiro, R. F. Caleya [(a)] and J. L. Santos [(b)]

Grupo de Optoelectrónica, INESC, R. José Falcão 110, 4000 Porto, PORTUGAL.

A number of optical and opto-electronic techniques have been developed for demodulation of interferometric fibre optic sensors. Some of these techniques include pseudo-heterodyne[1], phase-generated carrier (PGC) homodyne[2] and PGC synthetic heterodyne[3]. The two latter types of demodulation schemes provide the sensor information encoded on carrier signals (amplitude-modulated in the PGC homodyne case, and phase-modulated in the PGC synthetic-heterodyne case), and are suitable for use in conjunction with frequency or time division multiplexing topologies. In both of these techniques, the laser light source is frequency modulated by a sine wave with a predetermined amplitude (index modulation), so as to cause a sinusoidal phase modulation within the sensing interferometer. In this case, a known path imbalance must exist by construction of the interferometer, so that frequency variations of the light will cause a linearly proportional phase variation at the output of the sensor. When synthetic-heterodyne demodulation is used in an array of interferometric fibre sensors, and because, in practice, their path imbalances are different, the corresponding demodulated signals will be subject to amplitude and phase errors, due to misadjustments between the predetermined laser index modulation value and the path imbalance of each interferometer. These errors are investigated in this work, and it is shown how this problem can be attenuated.

Modulation of the laser frequency by applying a sinusoidal waveform, $\Delta i_m \sin \omega_m t$, to the injection current of the laser diode, gives rise to an interferometric phase modulation, $\Delta\phi$, at the output of an unbalanced interferometer, given by

$$\Delta\phi = \frac{2\pi n \Delta L}{c} \Delta i_m \frac{\delta\nu}{\delta i} \sin\omega_m t = \Delta\phi_m \sin\omega_m t \qquad (1)$$

where n is the mode effective refractive index, ΔL is the path imbalance, $\delta\nu/\delta i$ is the effective current-to-frequency conversion factor of the laser diode. A schematic diagram of the signal processing scheme is shown in Fig.1. Theoretical analysis indicates that if the laser amplitude modulation is adjusted such that $\Delta\phi_m$=2.6299 rad, then eq.(1) reduces to the form[4]

$$S_o\big|_{J_1=J_2} = \alpha I_o k J_1(\Delta\phi_m)\cos\left[\omega_c t + \phi(t)\right] \qquad (2)$$

where I_o is the optical input intensity, k is the fringe visibility, α is a constant factor taking into account the losses in the system, ω_c is an electronic generated frequency carrier, $J_a(\Delta\phi_m)$, a=0,1,2,..., are the first-kind Bessel functions, $\Delta\phi_m$ is the interferometric phase modulation due to the laser carrier (ω_m), and $\phi(t)$ is the output phase of the interferometer which contains the signal phase information of interest $\phi_s(t)$ and a drift component $\phi_d(t)$. From eq.(2) it is straightforward to recover the phase information $\phi_s(t)$, by using a frequency discriminator or a phase-locked loop (PLL) with subsequent integration. However, in an array of interferometric sensors it is not possible to fulfill the condition $\Delta\phi_m$=2.6299 rad, i.e., $J_1(\Delta\phi_m) = J_2(\Delta\phi_m)$, for all sensors in the network, because, in practice, their path imbalances cannot be identical (this means that, in general, the laser index modulation can only be adjusted each time to a single sensor in the network). Thus, when this condition $J_1(\Delta\phi_m) = J_2(\Delta\phi_m)$ is not fulfilled, equation (2) becomes

$$S_o\big|_{J_1\neq J_2} = \alpha I_o k J_1(\Delta\phi_m) F(\zeta_{21},\phi)\cos\left[\omega_c t + \alpha(\zeta_{21},\phi)\right] \qquad (3)$$

where,

$$F(\zeta_{21},\phi) = \sqrt{\frac{1+\zeta_{21}^2 - (1-\zeta_{21}^2)\cos(2\phi(t))}{2}} \qquad (4)$$

$$\alpha(\zeta_{21},\phi) = \tan^{-1}\left[\frac{1}{\zeta_{21}}\tan\phi(t)\right] \;;\; \zeta_{21} = \frac{J_2(\Delta\phi_m)}{J_1(\Delta\phi_m)} \qquad (5)$$

Using a PLL locked at the center frequency ω_c in order to process the signal (3) the resulting output intensity, $P_o(J_1\neq J_2)$, is given by

$$\begin{aligned} P_o\big|_{J_1\neq J_2} &= \alpha I_o k J_1(\Delta\phi_m)\frac{\partial\phi(t)}{\partial t} H(\zeta_{21},\phi) \\ &= P_o\big|_{J_1=J_2} H(\zeta_{21},\phi) \end{aligned} \qquad (6)$$

where

$$H(\zeta_{21},\phi) = F(\zeta_{21},\phi)\frac{1}{\zeta_{21}\cos^2\phi(t) + \frac{1}{\zeta_{21}}\sin^2\phi(t)} \qquad (7)$$

When $J_1(\Delta\phi_m) = J_2(\Delta\phi_m)$, $H(\zeta_{21},\phi)$=1 and the free of error demodulated phase signal is obtained. It is important to notice that $F(\zeta_{21},\phi)$ and $H(\zeta_{21},\phi)$ depends on the quasi-static phase $\phi_d(t)$, which changes randomly and, therefore, variable calibration errors will be introduced in the demodulated phase signal. To evaluate this effect, we define the error function, ε_{21}, as the relative deviation of $P_{o(J1\neq J2)}$ from the ideal case $P_{o(J1=J2)}$, giving

$$\begin{aligned} \varepsilon_{21}(\%) &= \left[\frac{P_o\big|_{J_1\neq J_2} - P_o\big|_{J_1=J_2}}{P_o\big|_{J_1=J_2}}\right]100\% = \\ &= \left[H(\zeta_{21},\phi) - 1\right]100\% \end{aligned} \qquad (8)$$

Fig. 2a shows this error function (8) versus the demodulated phase, $\phi(t)$, for deviations of $\pm 0.01\Delta\phi_{mo1}$, $\pm 0.05\Delta\phi_{mo1}$ and $\pm 0.1\Delta\phi_{mo1}$, which correspond to

relative deviations of ±1%, ±5% and ±10% from the optimum value $\Delta\phi_{mo1}$, respectively. This optimum value, where the error is zero (J_1=J_2, i.e., ζ_{21}=1) is $\Delta\phi_{mo1}$=2.6299 rad. It is interesting to notice that, the error functions associated with relative deviations of +1% and -1% are very similar; however, for the ±10% case, these functions diverge by as much as 7%. This effect is due to ratio ζ_{21}, which is highly asymmetric with respect of the optimum value $\Delta\phi_{mo1}$, as can be seen from Fig.3. This figure also shows other high-order ζ ratios. It is evident that for identical deviations from the optimum values $\Delta\phi_{moi}$ (i=1,2,...), the parameter $\zeta_{i+1,i}$ decreases relatively to the standard case, i=1. This means that, if instead the Bessel pair $\{J_1,J_2\}$ we use an high-order Bessel pair, such as, $\{J_i,J_{i+1}\}$, with i>1, the function $H(\zeta_{i+1,1},\phi)$ will be decreased and, the resulting output intensity (6) will be given by

$$P_o\Big|_{J_i=J_{i+1}} = P_o\Big|_{J_i=J_{i+1}} H(\zeta_{i+1,i},\phi) \qquad (9)$$

where the variables involved in this equation are identical to those defined in relations (3) and (4), only substituting the pair $\{J_1,J_2\}$ by the pair $\{J_i,J_{i+1}\}$. As an example, Fig. 2b shows the relative error, ε_{43}(%), corresponding to the Bessel pair $\{J_3,J_4\}$, as a function of the demodulate phase $\phi(t)$ for deviations from the optimum value $\Delta\phi_{mo3}$=4.8805 rad (when J_3=J_4 i.e., ζ_{43}=1) of $\pm0.01\Delta\phi_{mo1}$, $\pm0.05\Delta\phi_{mo1}$ and $\pm0.1\Delta\phi_{mo1}$, which are the same than the ones considered in Fig. 2a (these deviations correspond to relative deviations with respect to $\Delta\phi_{mo3}$ of ±0.5%, ±2.7% and ±5.4%, respectively). Comparing these two error functions (Fig. 2a and 2b), a deviation of $0.01\Delta\phi_{mo1}$ for the case $\{J_3,J_4\}$ gives a phase demodulated error 35% smaller than the solution $\{J_1,J_2\}$; and for a deviation of $0.1\Delta\phi_{mo1}$, the improvement is 40%. These two examples illustrate the advantages of processing high-order Bessel pairs $\{J_i,J_{i+1}\}$, with i>1.

A Mach-Zehnder interferometer with path imbalance of ≈3.83 cm, using standard singlemode optical fibre, was built to evaluate the function $F(\zeta_{21},\phi)$. The optical source was a semiconductor laser (Melles-Griot 06DLS407, λ=785 nm, temperature controlled), operated 20 mA above threshold, and with a measured effective frequency-to-current factor of 5.4 GHz/mA. The injection current of the laser was modulated by a sinewave with a frequency of 24 kHz and amplitude of Δi_m (Δi_{mo1} = 0.417 mA ⇒ $\Delta\phi_{mo1}$ = 2.6299 rad, i.e.,J_1=J_2). A PZT stretcher was mounted in one arm of the interferometer to induce the phase signal information, $\phi(t)$. This PZT was driven by a sawtooth waveform (frequency=30 Hz, amplitude=17 V) to sweep the interferometer over one fringe. The electronic carrier (ω_c) used in the heterodyne circuit was 10 kHz.

Figures 4a and 4b, show the output signal (S_o) as a function of time (which is proportional to $\phi(t)$), for 1% and 25% relative deviations of ζ from one, which is achieved by changing the optimum value of the modulation current (the optimum valueΔi_{mo1} = 0.417 mA). Fig.5 shows the theoretical error amplitude modulation, $J_1(\Delta\phi_m)F(\zeta_{21},\phi)$ for the same deviations, and it is evident a significant agreement with the experimental results of figures 4a and 4b. Thus, the results (2) and (3) can be used to quantify the readout phase error generated by this synthetic-heterodyne processing scheme. For a single interferometric sensor, this (variable) error can be virtually eliminated through proper adjustment of the laser diode index modulation. However, in an array of interferometric sensors powered by a single optoelectronic unit, these errors can not, in general, be avoided, because it is not possible practically to perform an equalization of the path imbalances for all sensors. As it was demonstrated by figures 2a and 2b, if instead of the Bessel functions pair $\{J_1,J_2\}$ we use high-order Bessel functions pairs, such as $\{J_3,J_4\}$, the readout errors can be sucessively decreased.

In conclusion, the synthetic-heterodyne demodulation technique, frequently used to demodulate the phase information of interferometric fibre optic sensors, was analyzed from the viewpoint of the readout errors generated when there is a mismatch from the ideal conditions. These errors were quantified and experimentally tested, and their implications on arrays of interferometric sensors demodulated using this technique were assessed.

(a) Dept. Electrónica, Univ. Alfonso X El Sábio, Av. Univ.1, 28691-Villanueva de la Cañada, Madrid, SPAIN.
(b) Also with: Lab. Física, Fac. Ciências da Univ. Porto, Pr. Gomes Teixeira, 4000 Porto, PORTUGAL.

[1] *D.A. Jackson et. al., Electr. Lett. 18, 1081 (1982).*
[2] *A. Dandridge et. al., J. Quantum Eletr. 18, 1647 (1982).*
[3] *J.H. Cole et. al., J. Quantum Eletron. 18, 694 (1982).*
[4] *A.C. Lewin et. al., IEE Proc. 132, no.5, 271 (1985).*

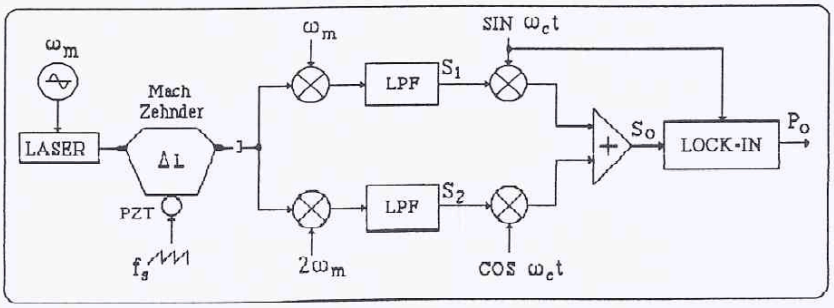

Fig.1. Schematic diagram of the synthetic-heterodyne demodulation scheme.

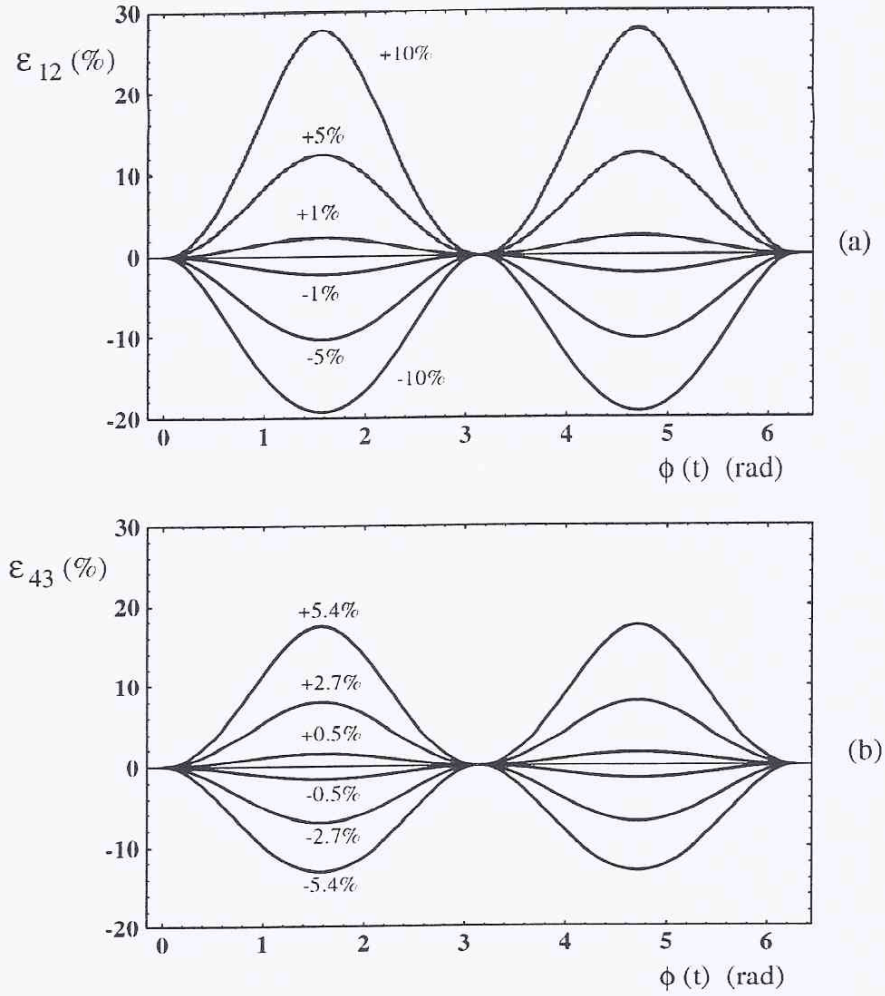

Fig.2 Error functions $\varepsilon_{i+1,1}$ (i=1,3) as a function of the demodulated phase $\phi(t)$, for deviations from the optimum values $\Delta\phi_{moi}$, of $\pm 0.01\Delta\phi_{mo1}$, $\pm 0.05\Delta\phi_{mo1}$ and $\pm 0.1\Delta\phi_{mo1}$; (a) Bessel pair $\{J_1,J_2\}$; (b) Bessel pair $\{J_3,J_4\}$.

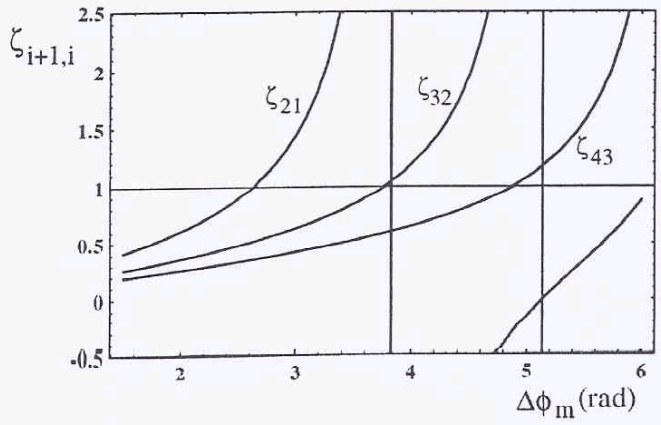

Fig.3 Ratios $\zeta_{i+1,i}$ (i=1,2,3) as a function of the amplitude modulation $\Delta\phi_m$.

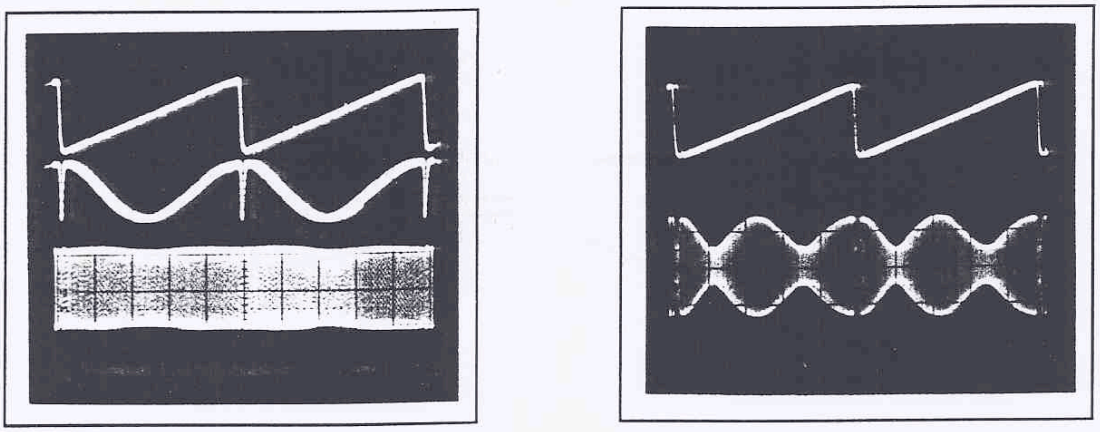

(a) (b)

Fig.4. Demodulated output signal S_o, (bottom trace) when the PZT is driven by the sawtooth (top trace) to sweep the interferometer over one fringe (middle trace) for (a) 1% and (b) 25% relative deviation of ζ_{21}.

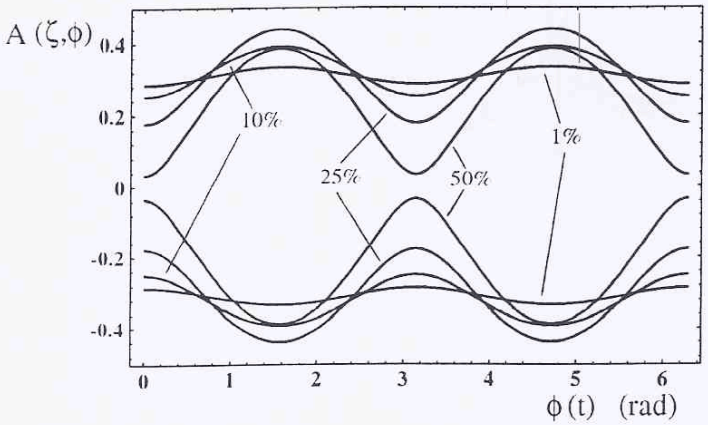

Fig.5. Error function $A(\zeta,\phi) = J_1(\Delta\phi_m)\ F(\zeta,\phi)$ versus phase $\phi(t)$ for different relative deviations of ζ_{21} from one.